*Date of Publication: 20th August 2026*
*ISSN: 2737-713X*

# GROUND SETTLEMENT ANALYSIS AT WASSA AGONA, GHANA, USING EMPIRICAL AND NUMERICAL METHODS

*[1] Jennifer Ama Dankwah, [1] Mawuko Luke Yaw Ankah, [1] Reuben Akwasi Frimpong

[1] *University of Mines and Technology, Tarkwa; P. O. Box 237, Tarkwa, Ghana - West Africa*
***Corresponding author:** mlyankah@umat.edu.gh

**Abstract**

*Ground settlement is a major issue in geotechnical engineering since it may cause significant structural damage and financial losses. The study evaluates ground settlement at Wassa Agona in the Western Region of Ghana using field investigation, laboratory testing and numerical methods. Five trial pits were investigated, from which soil samples were obtained for geotechnical characterisation and settlement assessment. Detailed data were gathered through fieldwork and laboratory testing, which provided the basis for empirical analysis and numerical modelling using Settle3D and Plaxis 3D software. The numerical settlement analysis was conducted under a foundation pressure of 125 kN/m$^2$ at 1.0 m embedment depth. Results from the laboratory and field tests revealed that the soil is mainly silt-dominated with low plasticity and specific gravity values indicating quartz-rich mineralogical setting. Oedometer consolidation test results indicated primary consolidation settlement values of 21.3 mm, 20.9 mm and 19.5 mm for Pit 1-Layer 3, Pit 2-Layer 3 and Pit 5-Layer 3, respectively. Settle3D predicted maximum staged settlement values of 34.1 mm, 30.4 mm and 36.1 mm, while Plaxis 3D predicted 10-year downward displacement values of 0.77 mm, 0.71 mm and 0.52 mm for the same pits, respectively. The results show that Settle3D is more responsive to one-dimensional compressibility and staged consolidation settlement, while Plaxis 3D provides a complementary three-dimensional finite element check on relative vertical displacement. The findings indicate that settlement serviceability checks should be included in foundation design at Wassa Agona, particularly where predicted staged settlements exceed acceptable limits.*

**Keywords**
Ground settlement, Consolidation settlement, Oedometer Test, Numerical modelling, Tropical soils

## Introduction

Settlement in geotechnical engineering is the downward vertical movement of ground or soil resulting from changes in internal stresses, usually caused by applied surface loads, excavation, groundwater variation or consolidation of compressible layers (Das, 2023; Terzaghi et al., 1996). In foundation engineering, settlement assessment is important because excessive total or differential settlement can reduce structural serviceability, induce cracking and compromise the long-term performance of buildings and other civil engineering structures (Elsharawy, 2024; Naghibi and Fenton, 2022). Reliable ground settlement assessment therefore requires site-specific soil characterisation, laboratory-based compressibility testing and appropriate interpretation of load-induced deformation.

Previous studies across West Africa have shown that foundation performance is strongly influenced by local soil conditions, geological setting and moisture-related changes in near-surface materials. In Tarkwa, Ghana, Tetteh et al. (2016) investigated foundation soils associated with a cracked building and showed the importance of test pits and laboratory soil characterisation in evaluating whether subsurface conditions contributed to structural distress. Similarly, Tuffour and Adom-Asamoah (2014) examined pre-compression parameters for accelerating consolidation settlement, emphasising the relevance of understanding primary consolidation behaviour before construction. In south-western Nigeria, Adebisi et al. (2018) combined geotechnical, chemical and oedometer consolidation testing to show that site-specific foundation design is necessary where compressibility and chemically aggressive soil conditions are present. Evinemi et al. (2016) also demonstrated that integrated geotechnical investigation can identify highly compressible layers responsible for structural subsidence in problematic ground conditions. These studies confirm the value of geotechnical investigation in foundation assessment. However, they also indicate that the use of laboratory-derived settlement results for validation of numerical settlement models has received limited attention in the reviewed West African literature.

In Ghana, settlement related studies have mostly focused on soil characterisation, building cracks, subsurface competence or general foundation conditions. While the existing Ghanaian studies provide useful evidence on the role of near-surface soils in structural performance, limited attention has been given to the cross-validation of oedometer-derived settlement values with numerical simulations from settlement and finite element modelling tools. This creates a practical gap because field and laboratory investigations provide direct measurements of soil behaviour at tested locations, but they do not always explain how settlement response may vary spatially under foundation loading. Numerical modelling, on the other hand, allows stress distribution, deformation patterns and foundation response to be examined under defined loading conditions (Ma et al., 2024). Combining empirical and numerical approaches therefore provides a stronger basis for checking settlement estimates, assessing load-induced deformation beyond individual sampling points, and identifying soil layers that may require improvement.

Wassa Agona was selected for this study because its geological and environmental conditions present practical foundation concerns that require local assessment. The area lies within the Tarkwa-Nsuaem Municipality, where mining activities, tropical rainfall and near-surface weathering can influence soil structure, moisture condition and compressibility. These conditions are important because settlement behaviour may vary where weathered fine-grained soils are present. The presence of perennial rivers, seasonal rainfall and disturbed land cover further supports the need for geotechnical evaluation before construction (Kumi-Boateng et al., 2012; Smith et al., 2016).

The novelty of this study lies in the integration of field and laboratory geotechnical characterisation, oedometer consolidation analysis, and numerical modelling using Settle3D and Plaxis 3D for ground settlement assessment at Wassa Agona. Unlike previous local studies that mainly focused on soil characterisation or structural cracking, this study compares empirical and numerical settlement outputs to evaluate the reliability of the predicted ground response under a defined foundation loading condition. The objectives of the study are therefore to: (a) characterise the geotechnical and chemical properties of soils at Wassa Agona; (b) determine the consolidation settlement behaviour of selected soil layers; (c) model immediate and long-term settlement response using Settle3D and Plaxis 3D; and (d) compare the laboratory-derived and numerical outputs to identify locations requiring careful foundation design or ground improvement.

## Materials and Methods

### Description of the study area

Wassa Agona is located within the Tarkwa-Nsuaem Municipality of Ghana's Western Region (Figure 1), positioned between latitude 5°13′00″ N and longitude 2°01′24″ W. The community occupies approximately 1.5 $km^2$ within the broader municipal area of 2,354 $km^2$ and is accessible by major highways and the national railway network linking Takoradi, Tarkwa and Kumasi. The area lies within the transition zone between the high rainforest and the Moist Semi-Deciduous Forest belt and is characterised by a tropical humid climate with a bimodal rainfall regime. Annual rainfall exceeds 1,750 mm, with major and minor wet seasons occurring from April to July and September to November, respectively. Mean daily temperatures range between 28°C and 33°C, while relative humidity typically exceeds 80% (Christiansen and Awadzi, 2000; Owusu-Bennoah et al., 2000).

The local terrain is characterised by northeast-southwest trending pitch-and-scarp slopes that form a sequence of parallel hills and valleys. The Huni and Bonsa Rivers define the boundaries of the locality and remain perennial, yet their reduced discharge in the dry season increases the likelihood of flooding during the wet months (Kuma et al., 2002; Obosu et al., 2019). The area formerly supported dense Mahogany, Sapele, Wawa and Odum-dominated forest, but intensive open-pit mining,

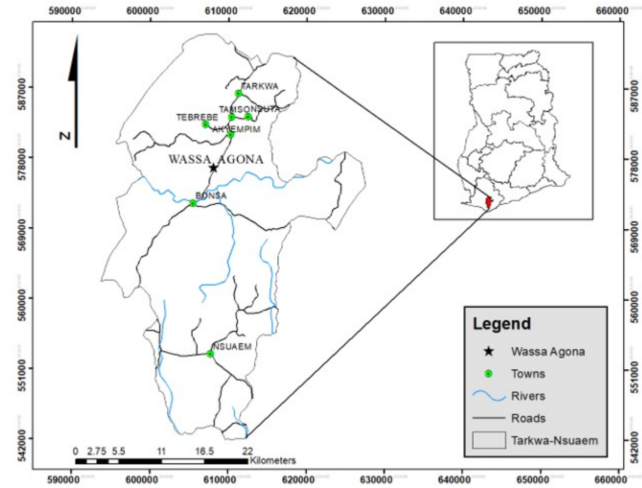


**Figure 1.** Location Map of the Study Area

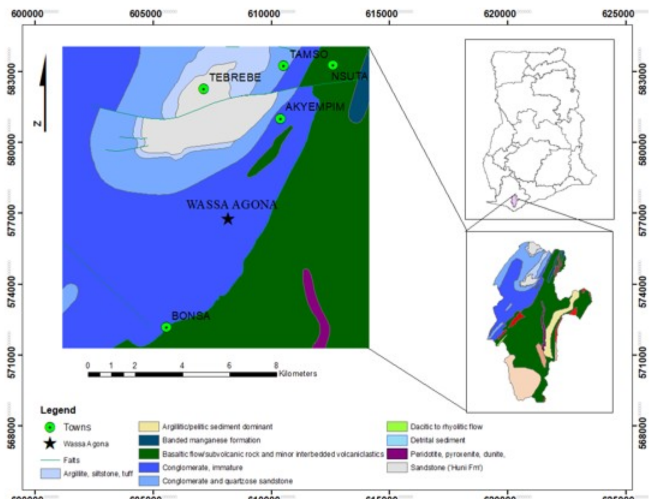


**Figure 2.** Geological Map of the Study Area

agriculture and timber extraction have substantially diminished vegetation cover, increasing ecological vulnerability and altering local environmental conditions (Kumi-Boateng et al., 2012).

Geologically, Wassa Agona lies within the Tarkwaian System, which unconformably overlies the Birimian Supergroup (Figure 2). The Tarkwaian rocks in the area comprise quartzites, sandstones, phyllites and conglomerates arranged within a narrow synclinal structure (Kortatsi and Quansah, 2004; Smith et al., 2016). The locality falls within the Kawere Formation, which is mainly composed of feldspathic quartzites, grits, breccias and conglomerates. These geological materials, together with tropical weathering and moisture variation, are relevant to the development of near-surface soils that may influence compressibility and settlement behaviour under foundation loading.

### Field investigation and sampling

Field investigation was conducted at Wassa Agona to characterise the near-surface soil conditions and obtain representative samples for laboratory testing and settlement assessment. Five trial pits were excavated across the study area. Each trial pit measured 20 m × 20 m in plan and was excavated to a depth of 5 m. The trial pit locations were selected after field reconnaissance to represent the proposed foundation zones, provide spatial coverage across the investigated area and capture observable variations in near-surface ground conditions. Samples were collected according to observed soil layers, with emphasis on materials relevant to foundation settlement assessment.

Disturbed, undisturbed and groundwater samples were collected according to the requirements of the laboratory tests. Disturbed samples were used for soil index and classification tests, while undisturbed samples from selected Layer 3 horizons were used for oedometer consolidation testing. Groundwater samples were obtained from Pit 3, Pit 4 and Pit 5 for sulphate and chloride analysis, while the groundwater condition in the Plaxis 3D model was represented using a water table positioned 1.0 m below ground surface. The subsurface profile was described from the trial pit observations using soil colour, texture, consistency and layer changes, while the selected Layer 3 materials were used for oedometer consolidation testing and numerical settlement modelling.

### Dynamic Cone Penetration Test (DCPT)

The DCPT was conducted in-situ to assess penetration resistance and bearing capacity variation with depth. The test followed standard dynamic probing procedures consistent with British Standard European Norm International Organization for Standardization (BS EN ISO) 22476-2:2005+A1:2011. The test point was prepared by exposing the ground surface and ensuring vertical penetration of the cone during testing. The test was conducted at the prepared test point, and cumulative cone penetration was recorded against the corresponding number of hammer blows. The Dynamic Penetration Index (DPI) was calculated using Equation 1:

$$DPI = \frac{\Delta P}{\Delta N} \tag{1}$$

where $\Delta P$ denotes the incremental penetration and $\Delta N$ denotes the number of hammer blows.

The DCPT values were used to evaluate changes in near-surface soil resistance with depth and to support the interpretation of allowable bearing capacity across the investigated profile. The results were also useful for identifying relatively stiff and weak zones that could influence shallow foundation performance.

### Chemical Test (Sulphate and Chloride)

Chemical testing was conducted on groundwater samples from Pit 3, Pit 4 and Pit 5 to determine sulphate and chloride concentrations. These ions were assessed because elevated sulphate and chloride levels may affect the durability of concrete and reinforcement in foundation works. The samples were analysed under laboratory conditions using United States Environmental Protection Agency (USEPA) Method 8051 for sulphate and USEPA Method 8113 for chloride. The groundwater samples were collected in clean sample containers and submitted for laboratory analysis. The measured concentrations were reported in parts per million (ppm) and interpreted for their potential to pose chemical durability risks to foundation materials. This test was relevant to the settlement assessment because chemically aggressive groundwater may influence the long-term performance of foundation concrete and embedded reinforcement, especially where shallow foundations are considered.

### Natural moisture content

The natural moisture content, commonly referred to as water content ($w$), was determined in accordance with BS 1377: Part 2:1990 to quantify the in-situ water content of the soil samples. Representative disturbed soil samples were placed in labelled moisture containers and weighed before drying. The samples were oven-dried at 105 to 110 °C for at least 24 hours and reweighed after cooling. The natural moisture content (%) was calculated using Equation 2:

$$w = \frac{M_2 - M_3}{M_3 - M_1} \times 100 \tag{2}$$

where $w$ represents the natural moisture content, $M_1$ denotes the mass of the empty container and lid (g), $M_2$ represents the mass of container, lid, and wet soil (g), and $M_3$ represents mass of container, lid, and oven-dried soil (g).

The moisture content values were used to assess the field moisture condition of the soils and to support the interpretation of plasticity, compressibility and settlement behaviour.

### Specific Gravity

The specific gravity ($G_s$) was determined in accordance with BS 1377: Part 2:1990 using the pycnometer method. The soil samples were oven-dried to remove moisture and passed through the 0.425 mm sieve before testing. A 50 g oven-dried sample was prepared, and representative portions were placed into pycnometers for the test. The $G_s$ was used to evaluate the relative density of the soil solids and to support the interpretation of soil composition and uniformity across the trial pits. The $G_s$ of the soil was calculated using Equation 3:

$$G_s = \frac{M_2 - M_1}{(M_4 - M_1) - (M_3 - M_2)} \tag{3}$$

where $M_1$ represents the mass of pycnometer with cork (g), $M_2$ represents the mass of pycnometer with cork and soil (g), $M_3$ represents the mass of pycnometer with cork, soil, and water (g), and $M_4$ represents the mass of pycnometer filled with water only (g).

### Particle Size Distribution

Particle size distribution was determined in accordance with BS 1377: Part 2:1990 to classify the soils and quantify the proportions of gravel, sand, silt and clay-sized particles (Dascalu et al., 2022). A 1000 g oven-dried soil sample was used for sieve analysis. The prepared sample was passed through a set of standard sieves arranged in decreasing aperture size, and the mass of soil retained on each sieve was recorded. The percentage of material retained on each sieve was calculated using Equation 4:

$$\text{Percentage retained} = \frac{M_s}{M_d} \times 100 \tag{4}$$

where $M_s$ denotes the mass of soil retained on the sieve (g) and $M_d$ denotes the mass of the total sample used (g).
The particle size distribution established the dominant soil fraction and supported the engineering classification of the investigated soils. This was important for interpreting drainage condition, compressibility and settlement susceptibility.

### Sedimentation

Sedimentation analysis was conducted in accordance with BS 1377: Part 2:1990 to determine the particle size distribution of the fine-grained fraction that could not be adequately characterised by sieve analysis alone. A 50 g oven-dried fine soil sample obtained from the sieve analysis was mixed with 125 ml of sodium hexametaphosphate solution and allowed to stand for 24 hours to ensure proper dispersion. The suspension was then transferred into a sedimentation cylinder and made up to the calibration mark with distilled water. Hydrometer and temperature readings were recorded at 2, 5, 15, 30, 60, 250, and 1440 minutes to capture the sedimentation behaviour of the fine particles. The sedimentation results were combined with the sieve analysis results to obtain a complete soil gradation curve. The sedimentation analysis was used to quantify the silt and clay fractions more accurately. This was relevant to the settlement assessment because the fine fraction influences drainage behaviour, moisture sensitivity and compressibility of the investigated soils.

### Atterberg Limit Test

The Atterberg limits were determined in accordance with BS 1377: Part 2:1990 to evaluate the consistency and plasticity characteristics of the fine-grained fraction of the soils. The soil samples were air-dried, gently broken down and passed through the 0.425 mm sieve before testing.
The liquid limit (LL) was determined using the Casagrande method. A 120 g portion of the prepared soil was mixed with water to form a uniform paste and tested using the liquid limit device. Moisture contents corresponding to different blow counts were determined, and the LL was obtained by plotting moisture content against the logarithm of blow counts and identifying the water content corresponding to 25 blows. The LL was used to assess the soil's tendency to change consistency with increasing moisture content and to support the interpretation of compressibility and moisture sensitivity.
The plastic limit (PL) was determined using portions of the prepared soil paste. The soil was rolled into threads of approximately 3 mm diameter until crumbling occurred. The moisture content at this condition was recorded as the PL. The test was repeated three times, and the average moisture content was recorded, and the PL was calculated using Equation 5:

$$PL = \frac{M_2 - M_3}{M_3 - M_1} \times 100 \tag{5}$$

The PL was used to define the lower moisture boundary of plastic behaviour and to support the classification of the fine-grained soil fraction.
The plasticity index (PI) was calculated as the difference between the LL and PL using Equation 6:

$$PI = LL - PL \tag{6}$$

The PI was used to assess the range of moisture content over which the soil behaves plastically. This parameter was relevant for evaluating moisture sensitivity, potential volume change and suitability of the soil for foundation support.

### Consolidation Test

The oedometer consolidation test was conducted to determine the settlement magnitude, consolidation rate and compressibility behaviour of selected soil layers under one-dimensional vertical loading conditions. The test was conducted in accordance with BS 1377: Part 5:1990. Undisturbed specimens from Pit 1-Layer 3, Pit 2-Layer 3 and Pit 5-Layer 3 were used because these layers formed the basis for the empirical settlement assessment and comparison with Settle3D and Plaxis 3D outputs.
The specimens were carefully trimmed into the consolidation ring to minimise disturbance and preserve the natural soil structure. The specimen diameter used in the oedometer test was 45 mm, while the initial specimen height was obtained from the consolidation ring measurement for each specimen. Before loading, the initial condition of each specimen was determined from its mass, dimensions, moisture content and specific gravity. These initial condition parameters were necessary because consolidation behaviour is controlled not only by the applied load, but also by the starting moisture state, density, void space and saturation condition of the soil.
The initial moisture content ($w_0$) was calculated to define the water condition of the sample before loading using Equation 7:

$$w_0 = \frac{M_i - M_d}{M_d} \times 100 \tag{7}$$

where $M_i$ is the initial mass of the specimen and $M_d$ is the oven-dried mass of the specimen.
The initial bulk density ($\rho_b$) and the initial dry density ($\rho_d$) were calculated using Equations 8 and 9 to describe the mass of the soil specimen per unit volume and the compactness of the specimen before loading. These parameters provide the basis for estimating the initial void ratio ($e_0$) using Equation 10:

$$\rho_b = \frac{M_i}{A \times H_0} \tag{8}$$

$$\rho_d = \frac{\rho_b}{1 + w_0} \tag{9}$$

$$e_0 = \frac{G_s \times \rho_w}{\rho_d} - 1 \tag{10}$$

where $A$ is the area of the consolidation ring, $H_0$ is the initial height of the sample specimen, $G_s$ is the specific gravity (Mg/m$^3$), and $\rho_w$ is the density of water. $e_0$ was calculated to define the initial volume of voids available for compression under applied vertical stress.

The initial degree of saturation ($S_{r0}$) was calculated using Equation 11 to indicate the extent to which the soil voids were filled with water before loading:

$$S_{r0} = \frac{w_0 \times G_s}{e_0} \times 100 \tag{11}$$

After the initial specimen properties were determined, the samples were subjected to incremental vertical pressures of 2.725, 5.45, 13.625, 27.25, 54.5, 109, 218 and 436 kPa. Settlement readings were recorded at 0, 6 and 15 seconds; 30 seconds; 1, 2, 4, 8, 15 and 30 minutes; and 1 hour after each load increment. For the final loading stage, readings were continued at 2, 4 and 24 hours to ensure that primary consolidation was achieved. The settlement-time readings were plotted against the square root of time to determine the rate of consolidation.

The coefficient of consolidation ($c_v$) was determined using Equation 12 to describe the rate at which consolidation settlement develops with time:

$$c_v = \frac{T_v \times d^2}{t_{90}} \tag{12}$$

where $T_v$ is the time factor for the selected degree of consolidation, $d$ is the drainage path length and $t_{90}$ is the time corresponding to the selected degree of consolidation. The $c_v$ values were reported as m$^2$/year.

The coefficient of volume compressibility ($m_v$) was calculated for each pressure increment using Equation 13 to quantify the volume change of the soil per unit increase in effective vertical stress:

$$m_v = \frac{\Delta e}{(1 + e_i)\Delta\sigma'} \tag{13}$$

where $m_v$ is the coefficient of volume compressibility, $\Delta e$ is the change in void ratio over the pressure increment, $e_i$ is the void ratio at the beginning of the pressure increment and $\Delta\sigma'$ is the change in effective vertical stress. The $m_v$ values were also used as input parameters in the numerical settlement modelling.

The void ratio-effective vertical stress relationship was developed from the oedometer loading and unloading stages to show how the soil compressed under increasing effective vertical stress. This relationship was used to interpret compressibility behaviour and to support the estimation of settlement-related parameters. Where the curve permitted, the compression index ($C_c$), recompression index ($C_r$) and preconsolidation pressure ($\sigma'_p$) were interpreted from the appropriate portions of the void ratio-effective stress relationship.

The consolidation analysis was therefore interpreted using settlement magnitude, $c_v$, $m_v$, $e_0$ and the void ratio-effective stress relationship, rather than settlement values alone. The oedometer-derived settlement and compressibility parameters were used as the empirical basis for comparison with Settle3D and Plaxis 3D settlement predictions.

## Numerical Methods

Numerical settlement modelling was conducted to evaluate the load-induced deformation response of the selected foundation soils and to compare the model predictions with the laboratory-derived consolidation behaviour. The numerical analysis focused on Pit 1-Layer 3, Pit 2-Layer 3 and Pit 5-Layer 3, because these layers provided the oedometer-derived compressibility parameters used for settlement interpretation. The same foundation pressure of 125 kN/m$^2$ at 1.0 m embedment depth was adopted in the numerical models to maintain consistency between the Settle3D and Plaxis 3D analyses.

The numerical input parameters were obtained from the laboratory consolidation results and related geotechnical interpretation, as illustrated in Table 1. The coefficient of earth pressure at rest ($K_0$) was estimated using Jaky's relationship, $K_0 = 1 - \sin\phi'$, where $\phi'$ is the effective friction angle (Jaky, 1944). The predicted settlements were then compared with the laboratory-derived settlement and compressibility behaviour to assess the consistency and engineering reliability of the numerical modelling approach.

### Settle3D

Settle3D was used to estimate the immediate and long-term consolidation settlement of the selected soil layers. The model was developed for Pit 1-Layer 3, Pit 2-Layer 3 and Pit 5-Layer 3 using the oedometer-derived parameters (Table 1).

The Settle3D analysis adopted a linear elastic $m_v$-based Terzaghi one-dimensional consolidation approach with Boussinesq stress distribution for a flexible rectangular foundation. The linear elastic component was used as a practical modelling simplification for estimating the immediate stress-settlement response from the available stiffness and compressibility parameters. This assumption was not treated as a complete description of soil behaviour, since natural soils can exhibit nonlinear and stress-dependent deformation. The time-dependent settlement response was therefore governed mainly by the oedometer-derived $m_v$ and $c_v$ values.

The model (Table 2) consisted of a single compressible layer of 2.5 m thickness for each pit location. Single drainage was assigned, with drainage permitted at the top surface only. The foundation was represented as a 20 m × 20 m rectangular loaded area subjected to 125 kN/m$^2$ at an embedment depth

**Table 1.** Geotechnical parameters used for numerical settlement modelling

| Parameter | Symbol/unit | Pit 1-L3 | Pit 2-L3 | Pit 5-L3 | Source |
|---|---|---|---|---|---|
| Young's modulus | E (kN/m$^2$) | 7,000 | 8,000 | 10,000 | Derived from $m_v$ |
| Effective Cohesion | $c'$ (kPa) | 15 | 16 | 18 | Estimated from PI |
| Effective Friction angle | $\phi'$ (°) | 26 | 26 | 27 | Estimated from PI |
| Coefficient of volume compressibility | $m_v$ (m$^2$/MN) | 0.085 | 0.109 | 0.136 | Oedometer test |
| Coefficient of consolidation | $c_v$ (m$^2$/year) | 0.389 | 0.072 | 0.136 | Oedometer test |
| Initial void ratio | $e_0$ | 0.296 | 0.325 | 0.282 | Oedometer test |
| Unit weight | $\gamma$ (kN/m$^3$) | 19 | 19 | 19 | Consolidation data |
| Coefficient of earth pressure at rest | $K_0$ | 0.56 | 0.56 | 0.55 | Jaky's formula |
| Interface reduction factor | $R_{inter}$ | 0.70 | 0.70 | 0.70 | Concrete on low-plasticity clay |

*Note:* The numerical input parameters were obtained from the laboratory consolidation results and related geotechnical interpretation.

**Table 2.** Settle3D model configuration

| Modelling aspect | Configuration |
|---|---|
| Software | Settle3D |
| Model approach | Linear elastic $m_v$-based Terzaghi one-dimensional consolidation |
| Stress distribution method | Boussinesq method for flexible foundation |
| Modelled locations | Pit 1-Layer 3, Pit 2-Layer 3 and Pit 5-Layer 3 |
| Compressible layer | Single compressible layer per pit |
| Compressible layer thickness | 2.5 m |
| Drainage condition | Single drainage, drained at top surface only |
| Foundation geometry | Rectangular foundation, 20 m × 20 m |
| Foundation pressure | 125 kN/m$^2$ |
| Embedment depth | 1.0 m |
| Time stages | 0, 0.5, 1, 5 and 10 years |
| Main input parameters | $m_v$, $c_v$, $e_0$, unit weight and stiffness from laboratory data |

of 1.0 m. Settlement was evaluated at 0, 0.5, 1, 5 and 10 years to capture the immediate and long-term settlement response under the applied foundation pressure.

For the primary consolidation component, Settle3D used the coefficient of volume compressibility to estimate settlement from the stress increase across the compressible layer. The consolidation settlement ($S_c$) was expressed using Equation 14:

$$S_c = m_v \times \Delta\sigma' \times H \tag{14}$$

where $m_v$ is the coefficient of volume compressibility (m$^2$/MN), $\Delta\sigma'$ is the increase in effective vertical stress (MN/m$^2$) and $H$ is the thickness of the compressible layer. The Settle3D outputs were interpreted as settlement predictions based on laboratory-derived compressibility parameters rather than as independently calibrated values. This allowed the model to complement the oedometer results and to assess how settlement may develop with time under the specified foundation pressure.

### Plaxis 3D

Plaxis 3D was used to model the three-dimensional deformation response of the selected pit locations under the same foundation pressure used in Settle3D. Three separate finite element models were developed for Pit 1-Layer 3, Pit 2-Layer 3 and Pit 5-Layer 3. The model domain measured 20 m × 15 m × 4 m, with a foundation pressure of 125 kN/m$^2$ applied at an embedment depth of 1.0 m.

The Mohr-Coulomb constitutive model (Table 3) was adopted with the Undrained B drainage option to represent short-term undrained soil response under foundation loading. This option was suitable because the model used effective stiffness parameters while accounting for pore-water pressure response during undrained loading. The model uses stiffness, unit weight, cohesion and friction angle to represent the deformation and shear strength response of the soil. This choice was appropriate for comparing relative settlement and displacement behaviour between pit locations under a defined loading condition, but it was not considered a full representation of nonlinear soil behaviour. The results were therefore interpreted within the limitations of the Mohr-Coulomb assumption.

The finite element mesh used 10-noded tetrahedral elements and was refined to a fine mesh quality. Boundary conditions were defined with a fixed base, roller sides and a free top surface. Positive interface elements were assigned between the foundation and soil using an interface reduction factor of 0.70. The water table was positioned 1.0 m below ground surface, consistent with the groundwater condition adopted in the Plaxis 3D model.

**Table 3.** Plaxis 3D model configuration

| Modelling aspect | Configuration |
|---|---|
| Software | Plaxis 3D |
| Constitutive model | Mohr-Coulomb with Undrained B drainage |
| Modelled locations | Pit 1-Layer 3, Pit 2-Layer 3 and Pit 5-Layer 3 |
| Model geometry | 20 m $\times$ 15 m $\times$ 4 m domain |
| Element type | 10-noded tetrahedral elements |
| Boundary conditions | Fixed base, roller sides and free top surface |
| Mesh quality | Fine mesh, 33,757 elements and 37,479 nodes |
| Interface condition | Positive interface elements, $R_{inter}$ = 0.70 |
| Water table | 1.0 m below ground surface |
| Foundation pressure | 125 kN/m$^2$ at 1.0 m embedment depth |
| Initial stress procedure | $K_0$ procedure |
| Loading phases | Footing installation and load application |
| Consolidation phase | 3,650 days, equivalent to 10 years |

The Plaxis 3D analysis used the $K_0$ initial stress procedure, followed by footing installation, foundation loading and a 3,650-day consolidation phase to assess time-dependent settlement. Model parameters were taken from the laboratory-derived and geotechnically interpreted values in Table 1, and the computed displacements were compared with the oedometer and Settle3D results.

## Results and Discussions

### Results

### Dynamic Cone Penetration Test (DCPT)

The DCPT results showed a steady increase in bearing capacity with depth, although local fluctuations occur within the profile. The average bearing capacity ($\bar{q}_u$) increased from 87 kPa at 10 cm to 1350 kPa at 330 cm, while the allowable bearing capacity ($q_a$) increased from 35 kPa to 540 kPa over the same depth interval. The initial increase in resistance indicates progressively stiffer near-surface materials, whereas the fluctuations observed after about 90 cm suggest changes in soil density, compaction and stratification. The DCPT trend is presented in Table 4 and Figure 3.

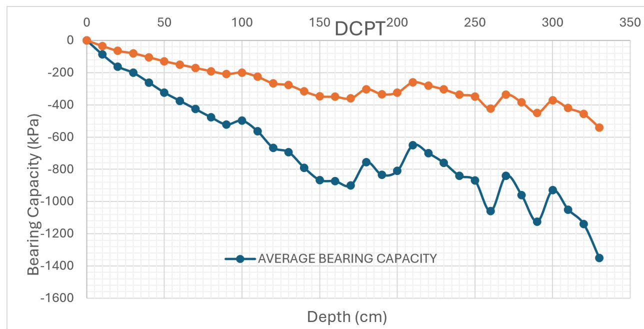


**Figure 3.** Graph of Average Bearing Capacity ($q_u$)/Allowable Bearing Capacity ($q_a$) Against Depth

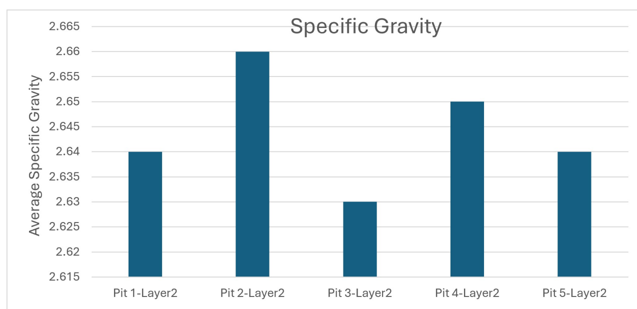


**Figure 4.** Specific Gravity Values of the Trial Pits

### Chemical Analysis (Sulphate and Chloride)

Groundwater chemistry varied across the sampled pits. Pit 4 recorded the highest chloride concentration (9.7 ppm), while Pit 5 recorded the highest sulphate concentration (35 ppm). Pit 3 exhibited the lowest concentrations for both parameters. The measured concentrations were generally low relative to thresholds commonly associated with aggressive chemical attack on concrete and embedded reinforcement in geotechnical practice. Nevertheless, the elevated sulphate at Pit 5 and chloride at Pit 4 indicate that groundwater chemistry should be considered during foundation concrete specification and material selection to ensure long-term durability.

### Specific Gravity ($G_s$)

$G_s$ values retrieved from all trial pits ranged between 2.63 and 2.66, indicating a uniform mineralogical composition dominated by quartz. These results reflect minimal spatial variation in soil density characteristics. The $G_s$ distribution is presented in Figure 4.

### Particle Size Distribution and Sedimentation

The particle size distribution results indicate that the investigated soils are dominated by silt, followed by sand, with a smaller clay fraction and trace gravel. The silt fraction ranged from 44.9% to 53.4%, the sand fraction ranged from 29.4% to 38.9%, and the clay content ranged from 11.5% to 18.3%. The

**Table 4.** Summary Results of the Dynamic Cone Penetration Test

| Depth (cm) | $\bar{q}_u$ (kN/m$^2$) | $q_a$ (kN/m$^2$) | Depth (cm) | $\bar{q}_u$ (kN/m$^2$) | $q_a$ (kN/m$^2$) |
|---|---|---|---|---|---|
| 0 | 0 | 0 | 170 | 900 | 360 |
| 10 | 87 | 35 | 180 | 756 | 302 |
| 20 | 162 | 65 | 190 | 834 | 334 |
| 30 | 201 | 80 | 200 | 810 | 324 |
| 40 | 261 | 104 | 210 | 650 | 260 |
| 50 | 324 | 130 | 220 | 700 | 280 |
| 60 | 375 | 150 | 230 | 760 | 304 |
| 70 | 426 | 170 | 240 | 840 | 336 |
| 80 | 477 | 191 | 250 | 870 | 348 |
| 90 | 522 | 209 | 260 | 1060 | 424 |
| 100 | 498 | 199 | 270 | 840 | 336 |
| 110 | 564 | 226 | 280 | 960 | 384 |
| 120 | 666 | 266 | 290 | 1125 | 450 |
| 130 | 693.33 | 277 | 300 | 930 | 372 |
| 140 | 790 | 316 | 310 | 1050 | 420 |
| 150 | 866.25 | 347 | 320 | 1140 | 456 |
| 160 | 873.75 | 350 | 330 | 1350 | 540 |

*Note:* $\bar{q}_u$ = Average bearing capacity; $q_a$ = Allowable bearing capacity.

**Table 5.** Summary of sulphate and chloride concentrations in groundwater

| Parameter | Sulphate (ppm) | Chloride (ppm) |
|---|---|---|
| Pit 3 Groundwater | <5 | <0.5 |
| Pit 4 Groundwater | 21 | 9.7 |
| Pit 5 Groundwater | 35 | <0.5 |

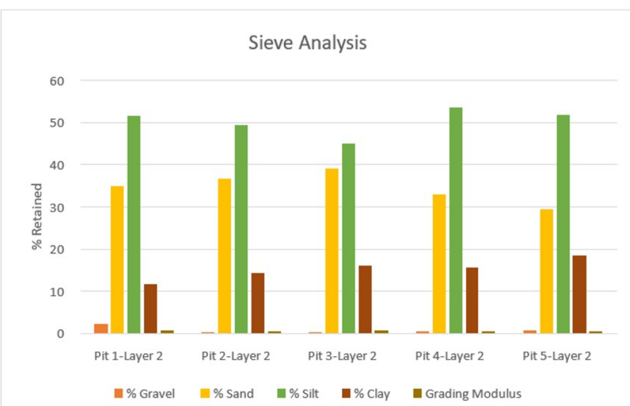


**Figure 5.** Particle Size Distribution and Sedimentation

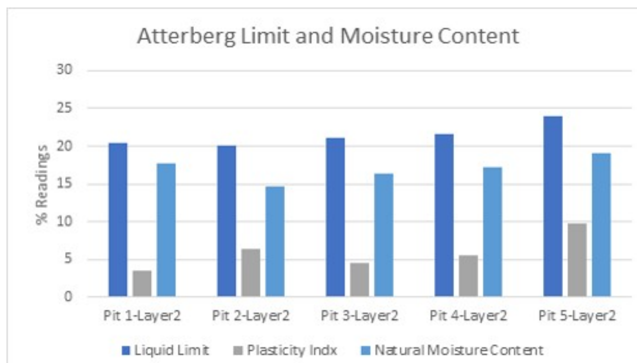


**Figure 6.** Atterberg Limits and Moisture Contents of the Various Pits

results in Figure 5 indicate that the fine fraction is sufficient to influence drainage and compressibility behaviour.

## Atterberg Limits and Natural Moisture Content

The LL values ranged from 20.1–23.9%, while PI varied between 3.4–9.8%. Natural moisture content values ranged from 14.7–19.14%. The low PI values (Figure 6) indicate low plasticity behaviour, while the natural moisture range shows that field moisture condition remains relevant to settlement and construction performance.

## Consolidation (Settlement Analysis)

The oedometer consolidation results were obtained for Pit 1-Layer 3, Pit 2-Layer 3 and Pit 5-Layer 3. The measured primary consolidation settlements were 21.275 mm, 20.905 mm and 19.505 mm, respectively. Although the settlement magnitudes were close, the compressibility parameters (Table 6) show that the selected layers do not behave identically under loading.

## Numerical Settlement Analysis (Settle3D)

Settle3D was used to evaluate total settlement for Pit 1-Layer 3, Pit 2-Layer 3 and Pit 5-Layer 3 under the applied foundation loading condition. In the Settle3D outputs, max (stage) represents the maximum settlement at the selected analysis stage, while max (all) represents the maximum settlement over all analysis stages. The difference between these two values shows the additional settlement that developed between the

**Table 6.** Summary Table of Consolidation Settlement Results

| Location | Oedometer settlement (mm) | $m_v$ ($m^2$/MN) | $c_v$ ($m^2$/year) | $e_0$ |
|---|---|---|---|---|
| Pit 1-Layer 3 | 21.275 | 0.085 | 0.389 | 0.296 |
| Pit 2-Layer 3 | 20.905 | 0.109 | 0.072 | 0.325 |
| Pit 5-Layer 3 | 19.505 | 0.136 | 0.136 | 0.282 |

*Note:* $m_v$ = Coefficient of volume compressibility; $c_v$ = Coefficient of consolidation; $e_0$ = Initial void ratio.

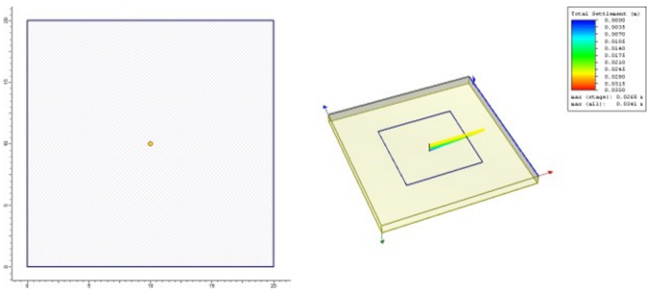

**Figure 7.** Settle3D Total Settlement Output of Pit 1-Layer 3

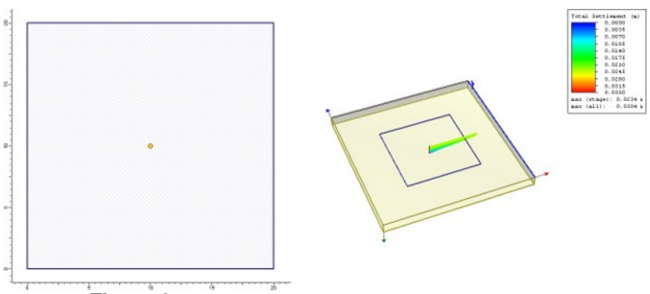

**Figure 8.** Settle3D Settlement Output of Pit 2-Layer 3

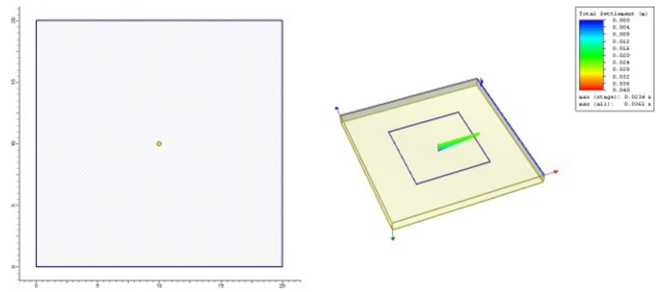

**Figure 9.** Settle3D Total Settlement Output of Pit 5-Layer 3

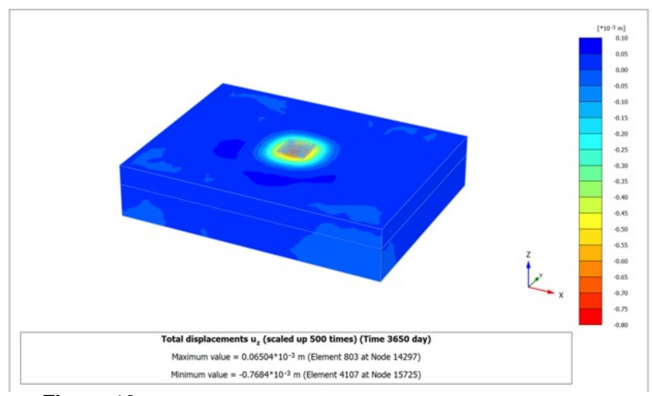


**Figure 10.** Plaxis 3D Total Displacement Output for Pit 1-Layer 3

selected stage and the maximum settlement recorded during the full staged analysis.

### Pit 1-Layer 3

The Settle3D output for Pit 1-Layer 3 showed a maximum settlement of 26.8 mm at the selected analysis stage and 34.1 mm over all analysis stages (Figure 7). This indicates that settlement increased by 7.3 mm across the staged analysis. The result shows that Pit 1-Layer 3 experienced a relatively high total settlement response, which is consistent with its lower stiffness.

### Pit 2-Layer 3

The Settle3D output for Pit 2-Layer 3 showed a maximum settlement of 23.4 mm at the selected analysis stage and 30.4 mm over all analysis stages (Figure 8). This indicates an additional staged settlement of 7.0 mm, showing that the layer continued to undergo compression across the modelled stages under the applied foundation load.

### Pit 5-Layer 3

The Settle3D output for Pit 5-Layer 3 showed a maximum settlement of 23.4 mm at the selected analysis stage and 36.1 mm over all analysis stages (Figure 9). This indicates an additional settlement of 12.7 mm, which was the highest increase among the three modelled layers. The result shows that this layer developed the greatest staged settlement increase, consistent with its higher coefficient of volume compressibility.

## Numerical Settlement Analysis (Plaxis 3D)

Plaxis 3D was used to evaluate the finite element total vertical displacement ($U_z$) response of Pit 1-Layer 3, Pit 2-Layer 3 and Pit 5-Layer 3 under the foundation pressure of 125 kN/$m^2$. In the Plaxis 3D output, the negative minimum $U_z$ values represent downward vertical displacement under the software sign convention; therefore, the settlement magnitudes were interpreted using the absolute values of the minimum $U_z$.

### Pit 1-Layer 3

The Plaxis 3D output for Pit 1-Layer 3 (Figure 10) showed a downward settlement of 0.7684 mm at 3650 days. This was the highest settlement among the three modelled layers, which is consistent with the relatively lower assigned Young's modulus and the corresponding parameter set used for this layer. The result indicates that the finite element response was mainly influenced by the lower stiffness condition.

**Table 7.** Quantitative comparison of oedometer settlement, Settle3D settlement outputs and Plaxis 3D vertical displacement

| Location | Oedometer settlement (mm) | Settle3D max (all) (mm) | Difference from oedometer (%) | Plaxis 3D downward displacement at 3650 days (mm) | Plaxis 3D rank |
|---|---|---|---|---|---|
| Pit 1-Layer 3 | 21.275 | 34.1 | 60.3 | 0.7684 | Highest |
| Pit 2-Layer 3 | 20.905 | 30.4 | 45.4 | 0.7111 | Intermediate |
| Pit 5-Layer 3 | 19.505 | 36.1 | 85.1 | 0.5178 | Lowest |

*Note:* The percentage differences show that Settle3D predicted higher settlement than the oedometer results. Plaxis 3D outputs represent 10-year vertical displacement from a stiffness-based three-dimensional finite element model.

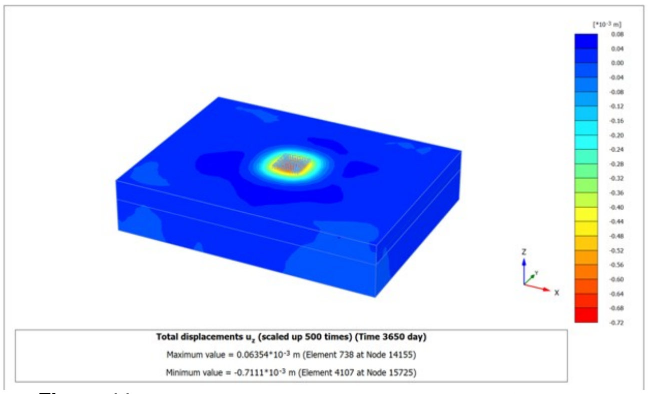


**Figure 11.** Plaxis 3D Total Displacement Output for Pit 2-Layer 3

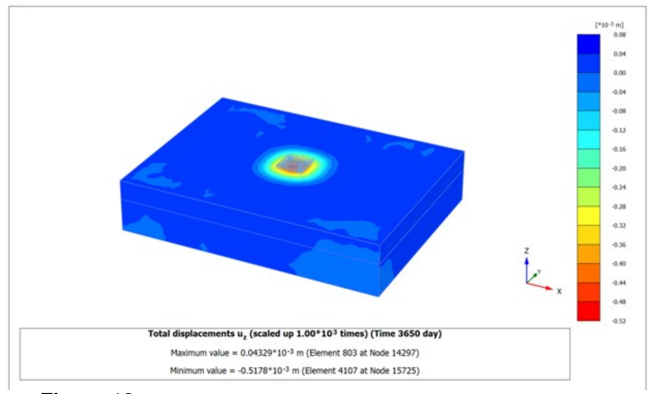


**Figure 12.** Plaxis 3D Total Displacement Output for Pit 5-Layer 3

### Pit 2-Layer 3

The Plaxis 3D output for Pit 2-Layer 3 (Figure 11) showed a downward settlement of 0.7111 mm at 3650 days. The slightly lower value reflects the combined influence of its stiffness, strength and initial stress parameters under the same foundation pressure. Although the layer had a relatively higher initial void ratio, the Plaxis 3D displacement response was governed more directly by the assigned stiffness and Mohr-Coulomb strength parameters.

### Pit 5-Layer 3

The Plaxis 3D output for Pit 5-Layer 3 (Figure 12) showed a downward settlement of 0.5178 mm at 3650 days. The lower settlement is consistent with the higher assigned stiffness of this layer, which reduced vertical deformation under the same loading condition.

### Numerical Comparison of Laboratory and Model Outputs

The percentage differences show that Settle3D predicted higher settlement than the oedometer results, particularly when the maximum settlement over all analysis stages was considered. The Plaxis 3D outputs were not expressed as percentage-error values against the oedometer settlements because they represent 10-year vertical displacement from a stiffness-based three-dimensional finite element model. Instead, the Plaxis 3D results are included to show the relative vertical displacement pattern under the same foundation pressure shown in (Table 7).

## Discussion

### Dynamic Cone Penetration Test (DCPT)

The DCPT trend indicates that penetration resistance improved with depth, although local fluctuations show that the near-surface soil strength varies within the investigated profile. Such variation is important because DCP resistance is commonly used to infer changes in in-situ soil strength and related engineering properties, including bearing resistance and stiffness (Keskin and Memis, 2025). The local fluctuations observed within the profile suggest alternating relatively stiff and weak zones, which should be considered in shallow foundation design because shallow penetration tests are useful for identifying near-surface stratigraphic changes (Navarrete et al., 2022). Therefore, the DCPT results support the need for controlled foundation embedment and site-specific settlement evaluation at Wassa Agona.

### Chemical Analysis of Groundwater

The elevated sulphate and chloride concentrations in Pit 4 and Pit 5 indicate that groundwater chemistry may influence the durability of foundation materials, not only the soil's settlement response. Sulphate exposure is relevant because it can promote expansive reactions and deterioration in cement-based materials (Zhang et al., 2024), while chloride ingress is widely associated with reinforcement corrosion in concrete (Ali et al., 2024). The relatively higher chloride value in Pit 4 therefore makes reinforcement protection important, whereas the sulphate levels in Pits 4 and 5 suggest that concrete specification should consider chemical exposure conditions. These findings support the need for durability-conscious foundation design at locations where groundwater interacts with concrete or embedded steel.

### Specific Gravity ($G_s$)

$G_s$ reflects the density of soil solids and is commonly linked to mineralogical composition in engineering soils. The range of values recorded across the trial pits indicates minimal variation in soil-solid characteristics and supports a broadly uniform mineralogical composition dominated by quartz. The quartz-rich nature of the soil suggests relatively stable soil-solid particles, meaning that the observed settlement differences are more likely controlled by soil fabric, initial void ratio and compressibility behaviour than by major mineralogical variation (Tiwari and Ajmera, 2011).

### Particle Size Distribution and Sedimentation

The particle size distribution and sedimentation results indicate that the investigated soils are mainly silt-dominated, with sand as the secondary fraction and minor clay content. This grading suggests that the soil behaviour is influenced strongly by the fine fraction, which can affect drainage, moisture retention and compressibility. The presence of silt and minor clay is therefore important for settlement assessment because fines can slow pore-water dissipation and increase sensitivity to load-induced compression (Fan et al., 2022). These results support the consolidation findings by showing that settlement behaviour at the site is controlled more by fine-grained soil fabric and compressibility than by coarse particle content alone.

### Atterberg Limits and Natural Moisture Content

The low LL and PI values indicate low-plasticity fine-grained soils with relatively low plastic deformation potential. This suggests a lower tendency for severe moisture-induced volume change, although the moderate natural moisture content suggests that compressibility may still develop in the silt-dominated layers under foundation loading (Bello et al., 2019; O'Kelly, 2021). These findings point to controlled foundation design and moisture management rather than outright rejection of the site, especially where settlement-sensitive layers are present.

### Consolidation Settlement

The oedometer results show that the selected Layer 3 materials are compressible under vertical loading, with settlement varying between the tested pits. This variation is meaningful because consolidation settlement depends on the void ratio-stress response, $c_v$ and $m_v$, not settlement magnitude alone (Shukla et al., 2009). The higher settlement rate recorded for Pit 2-Layer 3 indicates faster time-dependent compression, which makes it more critical for construction sequencing and settlement monitoring.

### Settle3D Settlement Response

The Settle3D results show that the maximum settlement over all analysis stages ranged from 30.4 to 36.1 mm, indicating that staged settlement is relevant to the shallow foundation response. These values exceed the commonly used 25 mm indicative serviceability benchmark for total settlement of shallow foundations, although the actual tolerable settlement depends on the structural type, stiffness and sensitivity to differential movement (BSI, 2015; Skempton and MacDonald, 1956). The difference between the selected-stage and all-stage settlement values shows that settlement continued to develop during the staged analysis, consistent with one-dimensional consolidation behaviour in which settlement magnitude is governed by compressibility, applied stress increase and compressible layer thickness (Terzaghi et al., 1996). Pit 5-Layer 3 produced the greatest staged settlement increase, which agrees with its higher coefficient of volume compressibility, and indicates greater susceptibility to compression under sustained loading. The Settle3D results indicate that shallow foundation design at the site should include serviceability settlement checks in addition to bearing capacity assessment. Where predicted settlements exceed acceptable limits, the applied foundation pressure should be controlled or ground improvement considered.

### Plaxis 3D Displacement Response

The Plaxis 3D results show a consistent reduction in 10-year downward settlement from Pit 1-Layer 3 to Pit 5-Layer 3, indicating that the finite element response was sensitive to the laboratory-derived stiffness and compressibility parameter set. The larger displacement at Pit 1-Layer 3 reflects the influence of its lower assigned Young's modulus, while the smaller displacement at Pit 5-Layer 3 is consistent with its higher stiffness and lower initial void ratio. Pit 2-Layer 3 produced an intermediate response, showing that its higher initial void ratio did not dominate the displacement pattern because the finite element response was governed more directly by the assigned stiffness and Mohr-Coulomb strength parameters. Practically, the results suggest that Pit 5-Layer 3 provides the most favourable deformation response under the applied foundation pressure, whereas Pit 1-Layer 3 requires closer attention in settlement-sensitive foundation design. These findings are consistent with the use of Mohr-Coulomb-type constitutive models for representing soil strength and stiffness response in finite element geotechnical analysis (Mohsan et al., 2021).

### Empirical and Numerical Settlement Comparison

The comparison shows that Settle3D predicted higher settlements than the oedometer test because the two methods represent different modelling conditions. The oedometer results were obtained from controlled one-dimensional laboratory specimens, whereas Settle3D applied the laboratory-derived compressibility parameters to a foundation-scale model with defined loading, stress distribution and compressible layer thickness. This explains why Settle3D produced larger staged settlement values, particularly where the coefficient of volume compressibility was higher.

Plaxis 3D was not compared with the oedometer results using percentage error because its output represents 10-year vertical displacement from a stiffness-based three-dimensional finite element model, not direct oedometer primary consolidation settlement. Its results are therefore better interpreted as a relative displacement pattern under the same foundation pressure. This distinction is important because Settle3D is more suitable for assessing serviceability settlement controlled by one-dimensional compressibility, while Plaxis 3D helps identify relative deformation response between the modelled pit locations.

Practically, the comparison shows that foundation design at Wassa Agona should not rely on a single settlement method. The oedometer and Settle3D results should guide serviceability settlement assessment, while the Plaxis 3D displacement pattern should support identification of zones requiring closer monitoring, foundation stiffening or ground improvement.

### Limitation of the study

This study presents an integrated field, laboratory and numerical assessment of ground settlement behaviour at Wassa Agona. However, some key limitations need to be acknowledged. The study was limited to five trial pits, so the results may not fully represent all subsurface variations across the construction site. The settlement assessment focused on selected Layer 3 materials, which means deeper or laterally variable soil layers were not fully evaluated. Some numerical modelling parameters were estimated from laboratory-derived and geotechnically interpreted variables, which may introduce uncertainty into the predictions. The study also did not include long-term field settlement monitoring to validate post-construction settlement behaviour. Future studies should include additional trial pits, deeper sampling intervals and wider spatial coverage to better capture lateral and vertical variations in subsurface conditions. Long-term field settlement monitoring and direct shear strength testing are also recommended to validate numerical predictions and improve the reliability of model input parameters.

## Conclusion

This study assessed ground settlement at Wassa Agona using field investigation, laboratory testing, oedometer consolidation analysis, Settle3D and Plaxis 3D. Five trial pits were investigated, and the numerical models were conducted under a foundation pressure of 125 kN/m$^2$ at 1.0 m embedment depth. The soils were mainly silt-dominated with low plasticity and relatively uniform specific gravity values, indicating a quartz-rich mineralogical setting. Settlement behaviour was controlled more by stiffness, void ratio and compressibility than by major variation in soil-solid composition. The oedometer tests confirmed primary consolidation settlement in Pit 1-Layer 3, Pit 2-Layer 3 and Pit 5-Layer 3, with settlement values of 21.275 mm, 20.905 mm and 19.505 mm, respectively. Settle3D predicted higher maximum staged settlements of 34.1 mm, 30.4 mm and 36.1 mm, showing that long-term serviceability settlement is important under the applied loading condition. Plaxis 3D predicted smaller 10-year downward displacements of 0.7684 mm, 0.7111 mm and 0.5178 mm, reflecting the stiffness-controlled vertical displacement response predicted by the three-dimensional finite element model. The empirical and numerical comparison showed that Settle3D captured foundation-scale staged settlement response, while Plaxis 3D described the relative finite element displacement pattern under the same foundation pressure. Pit 5-Layer 3 showed the most favourable oedometer and Plaxis 3D response, but its Settle3D staged settlement indicates that final foundation selection should still include serviceability settlement checks. Pit 1-Layer 3 requires closer monitoring or improvement because it recorded the highest oedometer settlement and Plaxis 3D downward displacement. Since the Settle3D settlements exceed the commonly used 25 mm indicative serviceability benchmark for shallow foundations, bearing capacity alone should not guide foundation design at the site. A raft foundation may be appropriate for the low-plasticity fine-grained profile because it can distribute load over a wider area and reduce differential settlement risk. Foundation design should include settlement serviceability checks, controlled foundation pressure and ground improvement or foundation stiffening where predicted settlements exceed acceptable limits.

## Acknowledgement

Special gratitude to Dr Yaw Osei Adutwum for sponsoring the university education of the first author.

## References

Adebisi, N., Osammor, J., and Oluwafemi, O. (2018). Chemical and geotechnical assessment of low organic foundation soils across the coastal area of Southwestern Nigeria. *Journal of African Earth Sciences*, 140:52–59. https://doi.org/10.1016/j.jafrearsci.2017.12.024.

Ali, M., Shams, M. A., Bheel, N., Almaliki, A. H., Mahmoud, A. S., Dodo, Y. A., and Benjeddou, O. (2024). A review on chloride induced corrosion in reinforced concrete structures: Lab and in situ investigation. *RSC Advances*, 14:37252–37271. https://doi.org/10.1039/D4RA03095E.

Bello, A. A., Owoseni, J. O., and Fatoyinbo, I. O. (2019). Evaluation of plasticity and consolidation characteristics of migmatite–gneiss-derived laterite soils. *SN Applied Sciences*, 1:934. https://doi.org/10.1007/s42452-019-0970-3.

BSI (2015). *BS 8004:2015 Code of practice for foundations*. British Standards Institution, London.

Christiansen, E. and Awadzi, T. (2000). Water balance in a moist semi-deciduous forest in Ghana. *West African Journal of Applied Ecology*, 1:11–22.

Das, B. M. (2023). *Principles of Foundation Engineering*. Cengage Learning, Boston, MA, 10th edition.

Dascalu, A.-V., Owusu-Yeboah, Z., Lungu, I., and Aniculaesi, M. (2022). The Influence of Dispersing Agents on Soil Particle Size Analysis. *Buletinul Institutului Politehnic din Iasi. Sectia Constructii, Arhitectura*, 68(4):125–140.

Elsharawy, M. (2024). The effect of 3D interference of shallow foundation on settlement and its impacts on building structures. *Civil Engineering and Architecture*, 12(3):2074–2090. https://doi.org/10.13189/cea.2024.120333.

Evinemi, I. E., Adepelumi, A. A., and Adebayo, O. (2016). Canal structure subsidence investigation using ground penetrating radar and geotechnical techniques. *International Journal of Geo-Engineering*, 7:9. https://doi.org/10.1186/s40703-016-0024-2.

Fan, J., Rowe, R. K., and Brachman, R. W. (2022). Compressibility and permeability of sand–silt tailings mixtures. *Canadian Geotechnical Journal*, 59(8):1348–1357. https://doi.org/10.1139/cgj-2021-0287.

Jaky, J. (1944). The coefficient of earth pressure at rest. *Journal of the Society of Hungarian Architects and Engineers*, 78(22):355–358.

Keskin, I. and Memis, M. A. (2025). Prediction of soil strength and dynamic properties through the dynamic cone penetration index. *Discover Civil Engineering*, 2:142. https://doi.org/10.1007/s44290-025-00142-0.

Kortatsi, B. and Quansah, J. (2004). Assessment of groundwater potential in the Sunyai and Techiman areas of Ghana for urban water supply. *West African Journal of Applied Ecology*, 5:22–30.

Kuma, J. S., Younger, P. L., and Bowell, R. J. (2002). Expanding the hydrogeological base in mining EIA studies: A focus on Ghana. *Environmental Impact Assessment Review*, 22(3):273–287. https://doi.org/10.1016/S0195-9255(02)00006-1.

Kumi-Boateng, B., Mireku-Gyimah, D., and Duker, A. (2012). A spatio-temporal based estimation of vegetation changes in the Tarkwa mining area of Ghana. *Research Journal of Environmental and Earth Sciences*, 4(3):215–229.

Ma, K., Gao, Z.-q., Wang, J., Zhang, Y., Zong, M.-f., Wu, W.-b., and Mei, G.-x. (2024). Nonlinear consolidation finite element analysis of a layered soft soil foundation under multistage loading based on the continuous drainage boundary. *Computers and Geotechnics*, 169:106220. https://doi.org/10.1016/j.compgeo.2024.106220.

Mohsan, M., Vardon, P. J., and Vossepoel, F. C. (2021). On the use of different constitutive models in data assimilation for slope stability. *Computers and Geotechnics*, 138:104332. https://doi.org/10.1016/j.compgeo.2021.104332.

Naghibi, F. and Fenton, G. A. (2022). Design of foundations against differential settlement. *Canadian Geotechnical Journal*, 59(3):384–396. https://doi.org/10.1139/cgj-2020-0614.

Navarrete, M. A. B., Breul, P., and Gourvès, R. (2022). Application of wave equation theory to improve dynamic cone penetration test for shallow soil characterisation. *Journal of Rock Mechanics and Geotechnical Engineering*, 14(1):289–302. https://doi.org/10.1016/j.jrmge.2021.05.007.

Obosu, J., Kuma, J., and Buah, W. (2019). Estimation of the quantity of water in the abandoned underground mine of Gold Fields Ghana Limited Tarkwa: a potential source to augment water supply to Tarkwa municipality. *Ghana Mining Journal*, 19(2):9–20. https://doi.org/10.4314/gm.v19i2.2.

O'Kelly, B. C. (2021). Review of recent developments and understanding of Atterberg limits determinations. *Geotechnics*, 1(1):59–75. https://doi.org/10.3390/geotechnics1010004.

Owusu-Bennoah, E., Awadzi, T., Boateng, E., Krogh, L., Breuning-Madsen, H., and Borggaard, O. (2000). Soil properties of a toposequence in the moist semi-deciduous forest zone of Ghana. *West African Journal of Applied Ecology*, 1:1–10.

Shukla, S., Sivakugan, N., and Das, B. (2009). Methods for determination of the coefficient of consolidation and field observations of time rate of settlement—an overview. *International Journal of Geotechnical Engineering*, 3(1):89–108. https://doi.org/10.3328/IJGE.2009.03.01.89-108.

Skempton, A. W. and MacDonald, D. H. (1956). The allowable settlements of buildings. *Proceedings of the Institution of Civil Engineers*, 5(6):727–768. https://doi.org/10.1680/ipeds.1956.12202.

Smith, A. J., Henry, G., and Frost-Killian, S. (2016). A review of the Birimian Supergroup-and Tarkwaian Group-hosted gold deposits of Ghana. *Episodes Journal of International Geoscience*, 39(2):177–197. https://doi.org/10.18814/epiiugs/2016/v39i2/95781.

Terzaghi, K., Peck, R. B., and Mesri, G. (1996). *Soil mechanics in engineering practice*. John Wiley & Sons, 3rd edition.

Tetteh, G. M., Mensah, F. A., and Ofosu, B. (2016). Foundation Soil Characterisation for a Building with Multiple Cracks at Tarkwa, Ghana. *Advances in Research*, 8(3):1–7. https://doi.org/10.9734/AIR/2016/29812.

Tiwari, B. and Ajmera, B. (2011). Consolidation and swelling behavior of major clay minerals and their mixtures. *Applied Clay Science*, 54(3-4):264–273. https://doi.org/10.1016/j.clay.2011.10.018.

Tuffour, Y. A. and Adom-Asamoah, M. (2014). Estimation of pre-compression parameters in the acceleration of consolidation settlement. Technical report, Department of Civil Engineering, KNUST.

Zhang, C., Li, J., Yu, M., Lu, Y., and Liu, S. (2024). Mechanism and performance control methods of sulfate attack on concrete: A review. *Materials*, 17(19):4836. https://doi.org/10.3390/ma17194836.